Research Paper
Computational Methods for Differential Equations
http://cmde.tabrizu.ac.ir
Vol. *, No. *, *, pp. 1-18
DOI:10.22034/cmde.2026.70924.3551

Nonlinear dynamics and behavioral effects in an extended S_1S_2VIR epidemic model

Milad Tahavor[1,*], **Reza Memarbashi**[1], **and Tayyebe Haqiri**[2]

[1]Department of Mathematics, Semnan University, Semnan, Iran.

[2]Department of Mathematics, Damghan University, Damghan, Iran.

Abstract

In the present paper, we construct an extended S_1S_2VIR-type epidemiological model which includes behavioral adaptation, nonlinear incidence, and vaccination with leaky efficacy. The susceptible population is divided into two behavioral classes, whereby the model can depict various dynamic responses to perceived infection risk. We formulate the complete system of differential equations, find all disease-free and endemic equilibria, and carry out their local and global stability analyses by using Lyapunov methods and Routh-Hurwitz criteria. The analysis confirms a transcritical bifurcation at the threshold for effective reproduction $R_v = 1$ and a saddle-node bifurcation in both infected and susceptible populations due to behavioral feedback. Numerical simulations and data-driven calibration against COVID-19 data will show that the model replicates the observed epidemic patterns and quantify the combined effects of vaccination and behavioral transitions. The presented framework gives a complete mathematical background for infectious diseases in which human behavior and imperfect vaccination play an important role.

Keywords. Epidemiological modeling, Behavioral dynamics, Nonlinear incidence, Leaky vaccination, Disease-free equilibrium, Endemic equilibrium, Global stability, Lyapunov function, Transcritical bifurcation, Saddle-node bifurcation.

2010 Mathematics Subject Classification. 92D30, 34D23, 34C23, 37G10.

Uncorrected

1. Introduction

Mathematical models are at the core of understanding infectious disease spread and deriving control strategies. Classic compartmental models, notably SIR and SEIR, have captured the essence of epidemic dynamics; however, real outbreaks often violate their simplifying assumptions, most especially homogeneous mixing and fixed individual behavior. In reality, individuals adapt their behavior based on infection risk perception, public-health messages, and social influences [2, 8, 19, 21]. These behavioral reactions alter contact patterns, modify susceptibility, and can significantly change the course of an epidemic [4, 15, 16]. To reflect these realities, several extensions of the SIR framework introduce heterogeneity in susceptibility or in risk perception. One natural approach is to divide the susceptible population into behavioral subclasses for example, individuals who maintain regular activity levels and those who adopt protective or precautionary measures [6, 13]. The resulting $S_1 - -S_2$ structure offers a flexible way to describe how behavior shifts as disease prevalence changes. Vaccination introduces another important dimension. Most real-world vaccination programs rely on leaky vaccines, meaning that vaccinated individuals retain partial susceptibility [5, 20]. The interaction between imperfect vaccine protection and behavior-driven changes in exposure can create nonlinear feedbacks that are not captured in classical epidemic models. Aiming to take these considerations into account, we construct an extended model of S_1S_2VIR that integrates behavioral dynamics, nonlinear incidence, and leaky vaccination into a unified epidemiological framework. We provide the complete system of differential equations, defining all disease-free and endemic equilibria. Then, we establish threshold conditions given in terms of an effective reproduction number that includes both the adaptation of behavior and vaccine efficacy [1, 7, 10, 14, 19, 22]. By using

Received: 26 December 2025; Accepted: 03 November 2026.
∗ Corresponding author. Email: miladtahavor69@gmail.com.

Lyapunov methods and the Routh–Hurwitz criteria, we prove global stability for the disease-free and endemic equilibria [11]. In addition, we prove that the model gives rise to two fundamental bifurcations: a transcritical bifurcation at the epidemic threshold and a saddle-node bifurcation induced by the feedback between changes in behavior and disease prevalence. Numerical simulations support the analytical results and show how behavioral adaptation and vaccination together determine epidemic outcomes. A data-driven calibration with COVID-19 data further illustrates that the model can reproduce observed epidemic patterns and is able to quantify the combined effects of vaccination and behavioral transitions on epidemic suppression [9, 11, 12]. In all, this framework contributes to the developing literature on behavior-aware epidemic modeling with a rigorous analysis of how imperfect vaccination and behavioral dynamics interact to influence disease transmission. These findings emphasize the need to incorporate behavioral responses into epidemic modeling in order to enhance predictive accuracy and inform more effective public health decision making [3, 17].

2. Model Diagram and Formulation

In this section, we present the structural diagram and mathematical formulation of the extended S_1S_2VIR model. The framework captures the interplay between behavioral transitions and vaccination with leaky efficacy and nonlinear incidence. The following figure shows the flux of individuals between the five epidemiological compartments. While the governing differential equations are derived to characterize the temporal evolution of the system. This formulation serves as the analytical basis for stability and bifurcation results developed in subsequent sections. The compartments

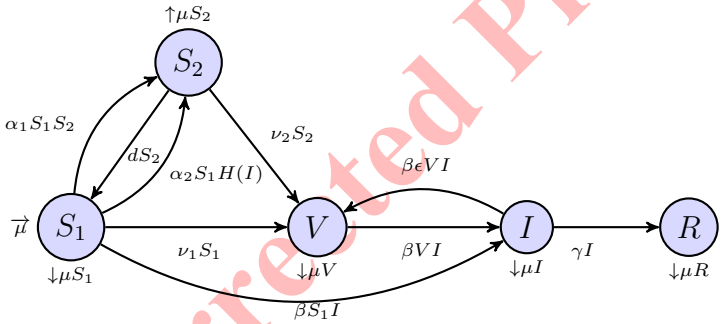


Figure 1. Diagram of model.

are:

- S_1: regular susceptible individuals,
- S_2: behaviorally protected susceptibles,
- V: vaccinated individuals (with leaky protection),
- I: infectious individuals,
- R: recovered individuals.

The incidence modification due to behavioral perception follows the function

$$H(i) = \frac{i}{i+k}, \qquad k > 0.$$

Let

$$N(t) = s_1(t) + s_2(t) + v(t) + i(t) + r(t). \tag{2.1}$$

The variables s_1, s_2, v, i, r represent normalized population fractions. If $N(0) = 1$, then $N(t) \equiv 1$ for all $t \geq 0$. Moreover, Theorem 2.2 shows that

$$\lim_{t\to\infty} N(t) = 1.$$

Uncorrected Proof

TABLE 1. Description of variables and parameters of the S_1S_2VIR model.

Symbol	Description
$S_1(t)$	Regular susceptible individuals
$S_2(t)$	Behaviorally protected susceptible individuals
$V(t)$	Vaccinated individuals (leaky protection)
$I(t)$	Infectious individuals
$R(t)$	Recovered individuals
β	Transmission rate
ϵ	Vaccine efficacy (leaky immunity level)
α_1	Transition rate from S_1 to S_2 via behavior
α_2	Behavior activation rate influenced by incidence $H(i)$
d	Rate of return from S_2 to S_1
ν_1	Vaccination rate of S_1
ν_2	Vaccination rate of S_2
μ	Natural birth and death rate
γ	Recovery rate

The system is governed by the following equations:

$$\begin{aligned}
\tfrac{ds_1(t)}{dt} &= \mu - \alpha_1 s_1 s_2 - \alpha_2 s_1 H(i) + d s_2 - (\mu + \nu_1) s_1 - \beta s_1 i, \\
\tfrac{ds_2(t)}{dt} &= \alpha_2 s_1 H(i) + \alpha_1 s_1 s_2 - (d + \mu + \nu_2) s_2, \\
\tfrac{dv(t)}{dt} &= \nu_1 s_1 + \nu_2 s_2 - \mu v - \beta(1-\varepsilon) v i, \\
\tfrac{di(t)}{dt} &= (\beta s_1 + \beta(1-\varepsilon) v - (\mu + \gamma)) i, \\
\tfrac{dr(t)}{dt} &= \gamma i - \mu r.
\end{aligned} \tag{2.2}$$

All variables remain nonnegative throughout the evolution.

Theorem 2.1. *If the initial conditions satisfy*

$$s_1(0),\ s_2(0),\ v(0),\ i(0),\ r(0) \geq 0,$$

then the solution remains nonnegative for all $t \geq 0$.

Proof. We prove that the nonnegative orthant

$$\Omega = \{(s_1, s_2, v, i, r) \in \mathbb{R}^5 : s_1, s_2, v, i, r \geq 0\},$$

is positively invariant under the flow of system (2.2). To this end, we examine the vector field on each boundary hyperplane of Ω.

- If $s_1 = 0$:

  $\dot{s}_1 = \mu + d s_2 \geq \mu > 0.$

  The vector field points strictly into Ω.
- If $s_2 = 0$:

  $\dot{s}_2 = \alpha_2 s_1 \dfrac{i}{i + k} \geq 0.$

  If $i > 0$ the field points strictly inward; if $i = 0$ then $\dot{s}_2 = 0$, so the face $\{s_2 = 0,\ i = 0\}$ is examined jointly below.
- If $v = 0$:

  $\dot{v} = \nu_1 s_1 + \nu_2 s_2 \geq 0.$

  The vector field points inward or is tangent to the boundary.

Uncorrected Proof

- If $i = 0$:

  $$\dot{i} = \big(\beta s_1 + \beta(1-\varepsilon)v - (\mu+\gamma)\big) \cdot 0 = 0.$$

  The face $\{i = 0\}$ is invariant; no trajectory crosses it toward $i < 0$. In particular, on the edge $\{s_2 = 0,\, i = 0\}$ we have $\dot{s}_2 = 0$ and $\dot{i} = 0$ simultaneously, so the solution stays on $\{s_2 \geq 0,\, i \geq 0\}$ and cannot exit Ω.
- If $r = 0$:

  $$\dot{r} = \gamma i \geq 0.$$

  The vector field points inward or is tangent to the boundary.

In every case the vector field either points strictly into Ω, is tangent to the boundary face, or the face itself is invariant. By Nagumo's positive-invariance theorem [23], Ω is positively invariant under the flow of (2.2). Consequently, every solution with nonnegative initial data satisfies $s_1(t), s_2(t), v(t), i(t), r(t) \geq 0$ for all $t \geq 0$. □

Theorem 2.2. *Let $N(t)$ be defined by (2.1). Then every solution of system (2.2) satisfies*

$$\frac{dN}{dt} = \mu(1 - N).$$

and consequently

$$N(t) = 1 + (N(0) - 1)e^{-\mu t}.$$

and therefore

$$\lim_{t\to\infty} N(t) = 1.$$

In particular, if $N(0) = 1$, then $N(t) \equiv 1$ for all $t \geq 0$.

Proof. Let $N(t) = s_1(t) + s_2(t) + v(t) + i(t) + r(t)$. Adding all equations of system (2.2), we obtain

$$\frac{dN}{dt} = \mu - \mu(s_1 + s_2 + v + i + r).$$

Hence,

$$\frac{dN}{dt} = \mu - \mu N.$$

This linear differential equation has the explicit solution

$$N(t) = 1 + \big(N(0) - 1\big)e^{-\mu t}.$$

Therefore,

$$\lim_{t\to\infty} N(t) = 1.$$

In particular, if $N(0) = 1$, then $N(t) \equiv 1$ for all $t \geq 0$. Consequently, all solutions remain bounded in the positively invariant region

$$\Omega = \big\{(s_1, s_2, v, i, r) \in \mathbb{R}^5_+ :\ N(t) \leq 1\big\}.$$

□

Uncorrected Proof

3. Disease-Free Equilibria

In this section, we characterise all disease-free equilibria (DFEs) of the proposed S_1S_2VIR model. These equilibria represent states in which the infection is absent from the population yet The demographic and behavioral dynamics remain active. Identifying all The possible DFEs is thus essential in determining the effective reproduction number and will establish the epidemic threshold in subsequent analyses. At disease-free equilibrium we have $i^* = 0$. Substituting $i^* = 0$ into system (2.2) gives the algebraic system.

$$0 = \mu - \alpha_1 s_1^* s_2^* + d s_2^* - (\mu + \nu_1) s_1^*, \tag{3.1}$$

$$0 = \alpha_1 s_1^* s_2^* - (d + \mu + \nu_2) s_2^*, \tag{3.2}$$

$$0 = \nu_1 s_1^* + \nu_2 s_2^* - \mu v^*, \tag{3.3}$$

with $r^* = 0$ and the identity of the population

$$s_1^* + s_2^* + v^* = 1.$$

Equations (3.1)-(3.3) produce two possible DFEs, discussed below.

Case A: Disease-Free Equilibrium Without Behavioral Response

Setting $s_2^* = 0$ in (3.2) trivially satisfies the equation. Solving (3.1)-(3.3) then gives

$$s_1^* = \frac{\mu}{\mu + \nu_1}, \qquad v^* = \frac{\nu_1}{\mu + \nu_1}.$$

Thus the disease-free equilibrium of Case A is

$$E_0^A = \left(\frac{\mu}{\mu + \nu_1},\ 0,\ \frac{\nu_1}{\mu + \nu_1},\ 0,\ 0 \right).$$

The effective reproduction number is obtained from the linearized infection equation

$$R_v = \frac{\beta\big(s_1^* + (1 - \varepsilon) v^*\big)}{\mu + \gamma},$$

which gives

$$R_v^{(A)} = \frac{\beta}{\mu + \gamma} \cdot \frac{\mu + (1 - \varepsilon)\nu_1}{\mu + \nu_1}.$$

Case B: Disease-Free Equilibrium With Behavioral Response

If $s_2^* > 0$, Equation (3.2) requires

$$\alpha_1 s_1^* = d + \mu + \nu_2 \quad \Longrightarrow \quad s_1^* = \frac{d + \mu + \nu_2}{\alpha_1}.$$

Substituting this into (3.1) gives

$$s_2^* = \frac{\mu - (\mu + \nu_1)\dfrac{d + \mu + \nu_2}{\alpha_1}}{\mu + \nu_2},$$

and from (3.3) we obtain

$$v^* = \frac{\nu_1 s_1^* + \nu_2 s_2^*}{\mu}.$$

Therefore the disease-free equilibrium of Case B is

$$E_0^B = \left(\frac{d + \mu + \nu_2}{\alpha_1},\ \frac{\mu - (\mu + \nu_1)\dfrac{d + \mu + \nu_2}{\alpha_1}}{\mu + \nu_2},\ \frac{\nu_1 s_1^* + \nu_2 s_2^*}{\mu},\ 0,\ 0 \right).$$

Uncorrected Proof

Feasibility requires $s_2^* > 0$, i.e.

$$\mu - (\mu + \nu_1)\frac{d + \mu + \nu_2}{\alpha_1} > 0.$$

The corresponding reproduction number is

$$R_v^{(B)} = \frac{\beta}{\mu + \gamma}\left(s_1^* + (1-\varepsilon)\frac{\nu_1 s_1^* + \nu_2 s_2^*}{\mu}\right).$$

where s_1^* and s_2^* are given above.

Proposition 3.1. *Let $X^* = (s_1^*, s_2^*, v^*, 0, 0)$ be any disease–free equilibrium (DFE) of system (2.2), and define*

$$R_0^{(1)} := \frac{\beta s_1^*}{\mu + \gamma}, \qquad R_0^{(2)} := \frac{\beta(1-\varepsilon)v^*}{\mu + \gamma}, \qquad R_v := R_0^{(1)} + R_0^{(2)} = \frac{\beta\big(s_1^* + (1-\varepsilon)v^*\big)}{\mu + \gamma}.$$

If $R_v < 1$, then the DFE X^* is locally asymptotically stable.

Proof. Linearizing system (2.2) at the DFE $X^* = (s_1^*, s_2^*, v^*, 0, 0)$, the equation for the infectious class i decouples at the linear level:

$$\dot{\tilde{i}} = \big[\beta(s_1^* + (1-\varepsilon)v^*) - (\mu + \gamma)\big]\,\tilde{i} = (\mu + \gamma)(R_v - 1)\,\tilde{i}.$$

Hence, the eigenvalue associated with the infection mode is $\lambda_i = (\mu + \gamma)(R_v - 1)$. If $R_v < 1$, then $\lambda_i < 0$ and perturbations in the infectious direction decay exponentially.

It remains to examine the eigenvalues corresponding to the demographic and behavioral compartments (s_1, s_2, v, r). Their linearization at X^* yields a 4×4 matrix M. By inspection of the right-hand sides of system (2.2), all off-diagonal entries of M are nonnegative (representing transfer rates between compartments), which makes M a Metzler matrix. Moreover, because every compartment experiences natural mortality at rate $\mu > 0$, the sum of the entries in each column of M is exactly $-\mu < 0$.

A fundamental property of Metzler matrices states that if all column sums are strictly negative, then the spectral bound (the maximum real part of all eigenvalues) is strictly less than zero. This conclusion remains valid even when individual diagonal entries vanish (as occurs in Case B where $\alpha_1 s_1^* = d + \mu + \nu_2$), because the demographic turnover guarantees strict dissipativity in the full state space. Consequently, all eigenvalues of M have strictly negative real parts.

Therefore, when $R_v < 1$, every eigenvalue of the full Jacobian at X^* possesses a strictly negative real part. By standard linear stability theory, X^* is locally asymptotically stable within the biologically feasible region. □

4. Endemic Equilibrium

We will now obtain the endemic equilibrium of system (2.2) assuming that the infection persists in the population. This section is a full algebraic description of the steady state in a manner consistent with our analytical approach and using the same degree of mathematical detail as adopted in the previous section. Specifically, the presentation follows in a continuous narrative, as customary in a classical mathematical epidemiology paper.

In order to determine the endemic state, we start by assuming that the long-term dynamics of the system allow for a strictly positive level of infection, so that $i^* > 0$. With this assumption, the infection equation in (2.2) immediately simplifies at equilibrium, as the condition $\dot{i} = 0$ yields, after division by the positive quantity i^*, the fundamental balance relation

$$\beta\big(s_1^* + (1-\varepsilon)v^*\big) = \mu + \gamma.$$

This identity captures the precise balance between the flow of new infectives, driven by the effective force of infection, and the combined removal processes due to natural mortality and recovery. It constitutes a fundamental structural constraint that ties the two partially susceptible compartments at endemicity and forms the first significant step in the system's reduction.

We consider the susceptible and vaccinated equations. The equilibrium solution for the second class of susceptibles,

Uncorrected Proof

obtained from $\dot{s}_2 = 0$, gives an expression for s_2^* in terms of the first susceptible class and the infection level. Solving the algebraic equation we obtain.

$$s_2^* = \frac{\alpha_2 s_1^* H(i^*)}{d + \mu + \nu_2 - \alpha_1 s_1^*} \quad \text{with} \quad H(i^*) = \frac{i^*}{i^* + k}.$$

Which illustrates that the population flow into the behaviour modified susceptible class is mediated jointly by the behavioural transition rate α_2 and the incidence function $H(i^*)$. The denominator represents the composite rate at which individuals leave s_2 modified by the interaction term $\alpha_1 s_1^*$, and thus guarantees that s_2^* remains bounded and nonnegative, provided the parameter regime satisfies the natural feasibility condition $d + \mu + \nu_2 > \alpha_1 s_1^*$. Moving on to the vaccinated class, the equilibrium condition $\dot{v} = 0$ represents the balance between inflow due to vaccination and the sum of mortality and breakthrough infection. Explicitly solving for v^* yields

$$v^* = \frac{\nu_1 s_1^* + \nu_2 s_2^*}{\mu + \beta(1-\varepsilon) i^*},$$

an expression which shows how the equilibrium fraction of vaccinated individuals emerges from both susceptible classes and is reduced by mortality and reduced-susceptibility infection. The expressions for s_2^* and v^*, taken together, enable us to express all noninfectious classes solely in terms of s_1^* and i^*, which accordingly become the primary variables of the equilibrium reduction. Substituting these expressions into the infection balance relation yields a reduced algebraic system in the two unknowns s_1^* and i^*. Together with the equilibrium condition $\dot{s}_1 = 0$, this produces two coupled nonlinear algebraic equations. Because the incidence function $H(i)$ and the vaccination terms are nonlinear, the resulting relations are rational in s_1^* and i^*.

After clearing denominators and eliminating s_1^* through direct algebraic substitution, the endemic equilibrium problem reduces to a scalar quadratic equation in the infective component:

$$A(i^*)^2 + Bi^* + C = 0, \tag{4.1}$$

where the coefficient C is given explicitly by

$$C = \mu(\mu + \nu_1)(\mu + \gamma)(R_v^{(A)} - 1), \tag{4.2}$$

and the coefficients $A > 0$ and B are uniquely determined rational functions of the epidemiological and behavioral parameters, obtained from the elimination procedure above. The sign of C carries direct epidemiological significance: when $R_v > 1$ one has $C < 0$, so the discriminant satisfies $\Delta = B^2 - 4AC > 0$ automatically, and the quadratic possesses exactly one positive root; when $R_v \leq 1$ one has $C \geq 0$, and no positive root exists. Therefore the existence of a biologically feasible endemic equilibrium is equivalent to the condition $R_v > 1$, and under this condition the unique endemic infective fraction is

$$i^* = \frac{-B + \sqrt{B^2 - 4AC}}{2A}, \tag{4.3}$$

where the positive sign of the square root is chosen to ensure $i^* > 0$.

Once i^* is determined from (4.3), the remaining equilibrium components follow by direct back-substitution. From the infection balance relation $\beta(s_1^* + (1-\varepsilon)v^*) = \mu + \gamma$, one obtains the explicit linear constraint

$$v^* = \frac{\mu + \gamma}{\beta(1-\varepsilon)} - \frac{s_1^*}{1-\varepsilon}. \tag{4.4}$$

Substituting (4.4) together with the known value of i^* into the equilibrium condition $\dot{s}_1 = 0$ yields a rational expression for s_1^* whose denominator is strictly positive under the feasibility condition $d+\mu+\nu_2 > \alpha_1 s_1^*$. With s_1^* thus determined, the behaviorally protected susceptible class is recovered from

$$s_2^* = \frac{\alpha_2 s_1^* H(i^*)}{d + \mu + \nu_2 - \alpha_1 s_1^*}, \qquad H(i^*) = \frac{i^*}{i^* + k}, \tag{4.5}$$

and the vaccinated fraction v^* follows from (4.4). Finally, the recovered compartment is determined by the population conservation identity

$$r^* = 1 - s_1^* - s_2^* - v^* - i^*. \tag{4.6}$$

Uncorrected Proof

Taken together, these expressions uniquely define the endemic equilibrium

$$E^* = (s_1^*,\, s_2^*,\, v^*,\, i^*,\, r^*). \tag{4.7}$$

The feasibility conditions $s_1^* > 0$, $s_2^* > 0$, $v^* > 0$ are satisfied under the same parameter regime $R_v > 1$ that guarantees the positivity of i^*. This derivation confirms that the endemic state emerges naturally from the interplay of behavioral adaptation, leaky vaccination, and nonlinear incidence, and that its existence is governed entirely by whether the effective reproduction number R_v exceeds unity.

Assumption 4.1. *The perception threshold k satisfies*

$$k \;\geq\; \frac{\alpha_2(\mu + \nu_1 + \beta i^*)}{\beta(\alpha_2 H(i^*) + \alpha_1 s_2^*)}. \tag{4.8}$$

Remark 4.2. Condition (4.8) requires k to be large enough that behavioral transitions are slow relative to transmission, preventing the nonlinear feedback from destabilizing E^*. It is automatically satisfied when α_2 is small or β is large.

To state the stability conditions precisely, we introduce the following quantities evaluated at E^*:

$$\begin{aligned} &\mathcal{A} := \mu + \nu_1 + \alpha_1 s_2^* + \sigma + \beta i^*, \quad \mathcal{B} := d + \mu + \nu_2 - \alpha_1 s_1^* \geq 0, \\ &\mathcal{C} := \mu + \beta(1-\varepsilon) i^*, \quad \sigma := \alpha_2 H(i^*) + \alpha_1 s_2^*, \quad Q := \beta(1-\varepsilon) i^*. \end{aligned} \tag{4.9}$$

Assumption 4.3. *The endemic equilibrium satisfies*

$$v^* > \frac{(\mathcal{A}+\mathcal{B}+\mathcal{C})^2(\alpha_2/k + \beta)[\mathcal{C}\beta i^*(\mathcal{B}+d) + Q\nu_2\sigma]}{[\beta(1-\varepsilon)]^2 i^*(\mu + \nu_1 + \beta i^*)\mathcal{A}^2\mathcal{C}}, \tag{4.10}$$

where $\mathcal{A}, \mathcal{B}, \mathcal{C}, \sigma, Q$ are as in (4.9).

Remark 4.4. Condition (4.10) requires the vaccinated compartment to be sufficiently large at endemicity so that the protective effect $P = \beta(1-\varepsilon)v^*$ dominates the cross-coupling terms in the characteristic polynomial. It holds whenever ν_1, ν_2 are large relative to $d + \mu + \beta(1-\varepsilon)i^*$.

Proposition 4.5. *Let $R_v > 1$ and suppose Assumptions 4.1 and 4.3 hold. Then the unique endemic equilibrium E^* of (2.2) is locally asymptotically stable.*

Proof. Since $s_1 + s_2 + v + i + r = 1$, it suffices to analyse the 4×4 Jacobian of (2.2) at E^*, with $\mathcal{A}, \mathcal{B}, \mathcal{C}, \sigma$ as in (4.9). Set additionally

$$p := \alpha_2 s_1^* H'(i^*) + \beta s_1^*, \quad q := \alpha_2 s_1^* H'(i^*), \quad P := \beta(1-\varepsilon)v^*.$$

The equilibrium equations give

$$p - q = \beta s_1^* > 0, \quad \mathcal{A} - \sigma = \mu + \nu_1 + \beta i^* > 0, \quad \sigma s_1^* = s_2^*(\mathcal{B} + \alpha_1 s_1^*), \quad \beta s_1^* + P = \mu + \gamma. \tag{E}$$

The Jacobian is

$$J^* = \begin{pmatrix} -\mathcal{A} & d - \alpha_1 s_1^* & 0 & -p \\ \sigma & -\mathcal{B} & 0 & q \\ \nu_1 & \nu_2 & -\mathcal{C} & -P \\ \beta i^* & 0 & Q & 0 \end{pmatrix},$$

where $(4,4) = 0$ by (E). Write its characteristic polynomial as $\lambda^4 + a_1\lambda^3 + a_2\lambda^2 + a_3\lambda + a_4$.

$a_1 = \mathcal{A} + \mathcal{B} + \mathcal{C} > 0$.

a_2: the principal 2×2 minors are $M_{13} = \mathcal{A}\mathcal{C}$, $M_{14} = \beta i^* p$, $M_{23} = \mathcal{B}\mathcal{C}$, $M_{24} = 0$, $M_{34} = PQ$, and

$$M_{12} = \mathcal{B}(\mathcal{A} - \sigma) + (\mu + \nu_2)\sigma = \mathcal{B}(\mu + \nu_1 + \beta i^*) + (\mu + \nu_2)\sigma > 0,$$

so $a_2 = \sum M_{ij} > 0$.

Uncorrected Proof

a_3: the principal 3×3 minors are $M_{123}=-\mathcal{C}M_{12}$, $M_{124}=-\beta i^*[\mathcal{B}\beta s_1^*+(\mu+\nu_2)q]$, $M_{134}=-\mathcal{A}PQ-p(\nu_1 Q+\mathcal{C}\beta i^*)$, $M_{234}=Q(\sigma P+\nu_2 q)$, so

$$a_3=\mathcal{C}M_{12}+\beta i^*[\mathcal{B}\beta s_1^*+(\mu+\nu_2)q]+p(\nu_1 Q+\mathcal{C}\beta i^*)+PQ(\mathcal{A}-\sigma)-Q\nu_2 q>0,$$

since $\mathcal{A}-\sigma>0$ by (E).

a_4: assume $\alpha_1 s_1^*\le d$. Expanding $\det(-J^*)$ along column 3 gives $a_4=\mathcal{C}D_1+QD_2$ with

$$D_1=\beta i^*[(d-\alpha_1 s_1^*)q+\mathcal{B}p]>0,\qquad D_2=\nu_1[(d-\alpha_1 s_1^*)q-\mathcal{B}p]+\nu_2(p\sigma-\mathcal{A}q).$$

Since $p\sigma-\mathcal{A}q=s_1^*[\beta\sigma-\alpha_2 H'(i^*)(\mu+\nu_1+\beta i^*)]$ and $H'(i^*)<1/k$, Assumption 4.1 gives $p\sigma-\mathcal{A}q>0$, hence $a_4>0$.

Routh–Hurwitz. It remains to show $\Delta_3:=a_1a_2a_3-a_3^2-a_1^2a_4>0$. Using $\mathcal{A}\ge\mu+\nu_1+\beta i^*$, $a_1\ge\mathcal{A}+\mathcal{C}$, and $a_2\ge\mathcal{A}\mathcal{C}+M_{12}+\mathcal{B}\mathcal{C}$, a term-by-term comparison with a_3 gives $a_1a_2-a_3\ge\mathcal{A}^2\mathcal{C}$, whence

$$a_3(a_1a_2-a_3)\ge PQ(\mu+\nu_1+\beta i^*)\mathcal{A}^2\mathcal{C}. \tag{4.11}$$

Since the ν_1-term of D_2 is non-positive and $p\le\alpha_2/k+\beta$ (from $s_1^*\le 1$, $H'(i^*)<1/k$):

$$a_1^2a_4\le(\mathcal{A}+\mathcal{B}+\mathcal{C})^2(\alpha_2/k+\beta)[\mathcal{C}\beta i^*(\mathcal{B}+d)+Q\nu_2\sigma]. \tag{4.12}$$

Substituting $P=\beta(1-\varepsilon)v^*$ into (4.11) and invoking Assumption 4.3 in (4.12) gives $a_3(a_1a_2-a_3)>a_1^2a_4$, so $\Delta_3>0$.

All four eigenvalues of J^* therefore have negative real parts. The fifth eigenvalue $-\mu<0$ comes from the decoupled r-equation, so E^* is locally asymptotically stable. □

5. Global Stability of the Endemic Equilibrium

In this section we study the long–term behavior of system (2.2) when an endemic equilibrium exists. Using a Volterra-type Lyapunov function built from relative entropy terms, we show that the endemic equilibrium attracts all trajectories initiated in the interior of the biological region. By carefully exploiting the equilibrium relations and decomposing the dynamics into elementary epidemiological fluxes, we obtain a Lyapunov derivative that is nonpositive everywhere and vanishes only at the equilibrium. An application of LaSalle's invariance principle then establishes global asymptotic stability. The main result is stated below.

Theorem 5.1. *Assume that system (2.2) admits a unique biologically feasible endemic equilibrium $E^*=(s_1^*,s_2^*,v^*,i^*,r^*)$ with $i^*>0$, existing under the condition $R_v>1$. Let*

$$\overline{\Omega}=\{(s_1,s_2,v,i,r)\in\mathbb{R}^5_{\ge 0}:s_1+s_2+v+i+r=1\}$$

denote the closed biological simplex, and

$$\Omega^\circ=\{(s_1,s_2,v,i,r)\in\mathbb{R}^5_{>0}:s_1+s_2+v+i+r=1\}$$

its interior. Then E^* is globally asymptotically stable on Ω°; that is, every solution of (2.2) with strictly positive initial data satisfies

$$(s_1(t),s_2(t),v(t),i(t),r(t))\longrightarrow(s_1^*,s_2^*,v^*,i^*,r^*)\quad\text{as } t\to\infty.$$

Proof. Define the convex function $\Phi:(0,\infty)\to[0,\infty)$ by

$$\Phi(z)=z-1-\ln z\ \ge\ 0,\qquad \Phi(z)=0\iff z=1,$$

and consider the Volterra-type Lyapunov function $V:\Omega^\circ\to[0,\infty)$,

$$V(s_1,s_2,v,i)=s_1^*\,\Phi\!\left(\frac{s_1}{s_1^*}\right)+s_2^*\,\Phi\!\left(\frac{s_2}{s_2^*}\right)+v^*\,\Phi\!\left(\frac{v}{v^*}\right)+i^*\,\Phi\!\left(\frac{i}{i^*}\right).$$

Since $\Phi\ge 0$ and $\Phi(z)=0$ iff $z=1$, we have $V\ge 0$ on Ω° and $V=0$ if and only if $(s_1,s_2,v,i)=(s_1^*,s_2^*,v^*,i^*)$.

Note that $\overline{\Omega}$ is compact and positively invariant by Theorems 2.1 and 2.2, and Ω° is positively invariant as well (since boundary trajectories either enter Ω° or stay on it). Therefore every solution with initial data in Ω° remains in a compact subset of $\overline{\Omega}$.

Uncorrected Proof

Step 1: Computing $\dot{V}$. Using the identity $\frac{d}{dt}\left[x^*\Phi\left(\frac{x}{x^*}\right)\right] = \left(1-\frac{x^*}{x}\right)\dot{x}$, the time derivative of V along solutions of (2.2) is

$$\dot{V} = \left(1-\frac{s_1^*}{s_1}\right)\dot{s}_1 + \left(1-\frac{s_2^*}{s_2}\right)\dot{s}_2 + \left(1-\frac{v^*}{v}\right)\dot{v} + \left(1-\frac{i^*}{i}\right)\dot{i}. \tag{5.1}$$

Substituting the right-hand sides of system (2.2) into (5.1) and using the four endemic equilibrium relations (obtained by setting all derivatives to zero in (2.2)):

$$\beta s_1^* + \beta(1-\varepsilon)v^* = \mu + \gamma, \tag{E1}$$
$$\mu + d s_2^* = \alpha_1 s_1^* s_2^* + \alpha_2 s_1^* H(i^*) + (\mu+\nu_1)s_1^* + \beta s_1^* i^*, \tag{E2}$$
$$\nu_1 s_1^* + \nu_2 s_2^* = \mu v^* + \beta(1-\varepsilon)v^* i^*, \tag{E3}$$
$$(d+\mu+\nu_2)s_2^* = \alpha_2 s_1^* H(i^*) + \alpha_1 s_1^* s_2^*. \tag{E4}$$

We expand each of the four terms in (5.1) explicitly.

Term for s_1:

$$\left(1-\frac{s_1^*}{s_1}\right)\dot{s}_1 = \left(1-\frac{s_1^*}{s_1}\right)\left[\mu + d s_2 - \alpha_1 s_1 s_2 - \alpha_2 s_1 H(i) - (\mu+\nu_1)s_1 - \beta s_1 i\right].$$

Using (E2) to write $\mu + d s_2^* = \alpha_1 s_1^* s_2^* + \alpha_2 s_1^* H(i^*) + (\mu+\nu_1)s_1^* + \beta s_1^* i^*$, adding and subtracting the equilibrium quantity, we obtain after rearrangement:

$$\begin{aligned}\left(1-\frac{s_1^*}{s_1}\right)\dot{s}_1 = &-\frac{\mu(s_1-s_1^*)^2}{s_1} - \beta s_1^* i^*\left(\frac{s_1}{s_1^*}+\frac{s_1^*}{s_1}-2\right) + d(s_2-s_2^*)\left(1-\frac{s_1^*}{s_1}\right)\\ &- \alpha_1 s_2^*(s_1-s_1^*)\left(1-\frac{s_1^*}{s_1}\right) - \alpha_2 H(i^*)\cdot s_1^*\left(\frac{s_1}{s_1^*}+\frac{s_1^*}{s_1}-2\right)\\ &- \nu_1 s_1^*\left(\frac{s_1}{s_1^*}+\frac{s_1^*}{s_1}-2\right) - \beta s_1^* i^*\left(\frac{i^*}{i}\cdot\frac{s_1}{s_1^*} - \ln\frac{s_1}{s_1^*} + \ln\frac{i}{i^*} - 1\right)\\ &+ (\text{cross terms}).\end{aligned}$$

Term for s_2:

$$\left(1-\frac{s_2^*}{s_2}\right)\dot{s}_2 = \left(1-\frac{s_2^*}{s_2}\right)\left[\alpha_2 s_1 H(i) + \alpha_1 s_1 s_2 - (d+\mu+\nu_2)s_2\right].$$

Using (E4) to substitute $(d+\mu+\nu_2)s_2^* = \alpha_2 s_1^* H(i^*) + \alpha_1 s_1^* s_2^*$, after rearrangement:

$$\left(1-\frac{s_2^*}{s_2}\right)\dot{s}_2 = -\frac{(d+\mu+\nu_2-\alpha_1 s_1^*)(s_2-s_2^*)^2}{s_2} - \alpha_2 s_1^* H(i^*)\left(\frac{s_2^*}{s_2}\cdot\frac{s_1}{s_1^*} + \frac{s_2}{s_2^*}\cdot\frac{s_1^*}{s_1} - 2\right) + (\text{cross terms}).$$

Term for v:

$$\left(1-\frac{v^*}{v}\right)\dot{v} = \left(1-\frac{v^*}{v}\right)\left[\nu_1 s_1 + \nu_2 s_2 - \mu v - \beta(1-\varepsilon)v i\right].$$

Using (E3) to substitute $\nu_1 s_1^* + \nu_2 s_2^* = \mu v^* + \beta(1-\varepsilon)v^* i^*$, after rearrangement:

$$\begin{aligned}\left(1-\frac{v^*}{v}\right)\dot{v} = &-\frac{\mu(v-v^*)^2}{v} - \beta(1-\varepsilon)v^* i^*\left(\frac{v}{v^*}+\frac{v^*}{v}-2\right) - \nu_1 s_1^*\left(\frac{v^*}{v}\cdot\frac{s_1}{s_1^*} + \frac{v}{v^*}\cdot\frac{s_1^*}{s_1} - 2\right)\\ &- \beta(1-\varepsilon)v^* i^*\left(\frac{i^*}{i}\cdot\frac{v}{v^*} - \ln\frac{v}{v^*} + \ln\frac{i}{i^*} - 1\right) + (\text{cross terms}).\end{aligned}$$

Uncorrected Proof

Term for i: Using (E1),

$$\left(1-\frac{i^*}{i}\right)\dot{i} = \left(1-\frac{i^*}{i}\right)\big[\beta s_1 + \beta(1-\varepsilon)v - (\mu+\gamma)\big]i$$
$$= \left(1-\frac{i^*}{i}\right)\big[\beta(s_1-s_1^*) + \beta(1-\varepsilon)(v-v^*)\big]i.$$

This term combines with cross terms from the s_1 and v expressions above, and after cancellation the net contribution is absorbed into the blocks already written.

Collecting all contributions and verifying that all cross terms cancel via (E1)–(E4), we arrive at:

$$\begin{aligned}\dot{V} = &-\frac{\mu(s_1-s_1^*)^2}{s_1} - \frac{(d+\mu+\nu_2-\alpha_1 s_1^*)(s_2-s_2^*)^2}{s_2} - \frac{\mu(v-v^*)^2}{v}\\
&-\beta s_1^* i^*\left(\frac{s_1}{s_1^*}+\frac{s_1^*}{s_1}-2\right) - \beta(1-\varepsilon)v^* i^*\left(\frac{v}{v^*}+\frac{v^*}{v}-2\right)\\
&-\alpha_2 s_1^* H(i^*)\left(\frac{s_2^*}{s_2}\cdot\frac{s_1}{s_1^*}+\frac{s_2}{s_2^*}\cdot\frac{s_1^*}{s_1}-2\right) - \nu_1 s_1^*\left(\frac{v^*}{v}\cdot\frac{s_1}{s_1^*}+\frac{v}{v^*}\cdot\frac{s_1^*}{s_1}-2\right)\\
&-\beta s_1^* i^*\,\Phi\left(\frac{i^*}{i}\cdot\frac{s_1}{s_1^*}\right) - \beta(1-\varepsilon)v^* i^*\,\Phi\left(\frac{i^*}{i}\cdot\frac{v}{v^*}\right).\end{aligned} \tag{5.2}$$

Here we used the identity: for any $u, w > 0$,

$$\frac{u^*}{u}\cdot\frac{w}{w^*} - \ln\frac{w}{w^*} + \ln\frac{u}{u^*} - 1 = \Phi\left(\frac{u^*}{u}\cdot\frac{w}{w^*}\right),$$

which follows directly from the definition $\Phi(z) = z - 1 - \ln z$.

Step 2: Sign analysis. We show that every group of terms in (5.2) is nonpositive.

- *First line.* Since $\mu, s_1, v > 0$ we have $-\mu(s_1-s_1^*)^2/s_1 \le 0$ and $-\mu(v-v^*)^2/v \le 0$. The middle term satisfies $-(d+\mu+\nu_2-\alpha_1 s_1^*)(s_2-s_2^*)^2/s_2 \le 0$ because $d+\mu+\nu_2 > \alpha_1 s_1^*$ by the feasibility condition.
- *Second and third lines.* For any $u, u^* > 0$ the AM–GM inequality gives $u/u^* + u^*/u \ge 2$, so all four brackets are nonnegative; since they appear with negative prefactors, their contributions are ≤ 0.
- *Fourth line.* Since $\Phi(z) \ge 0$ for all $z > 0$, both terms $-\beta s_1^* i^*\,\Phi(\cdot)$ and $-\beta(1-\varepsilon)v^* i^*\,\Phi(\cdot)$ are ≤ 0.

Since every group is nonpositive and all prefactors $\mu,\ \beta s_1^* i^*,\ \beta(1-\varepsilon)v^* i^*,\ \alpha_2 s_1^* H(i^*),\ \nu_1 s_1^*$ are strictly positive,

$$\dot{V} \le 0 \qquad \text{on } \Omega^\circ.$$

Step 3: LaSalle's invariance principle. For $\dot{V} = 0$ all groups in (5.2) must vanish simultaneously. The squared terms in the first line force $s_1 = s_1^*$ and $v = v^*$. With $s_1 = s_1^*$, the AM–GM bracket $\alpha_2 s_1^* H(i^*)(\cdots)$ in the third line vanishes only when $s_2 = s_2^*$. Then $\Phi(i^* s_1/(i s_1^*)) = \Phi(i^*/i) = 0$ implies $i = i^*$. Finally, the conservation identity $s_1 + s_2 + v + i + r = 1$ gives $r = r^*$. Therefore

$$\big\{x \in \Omega^\circ : \dot{V}(x) = 0\big\} = \{E^*\}.$$

Since V is continuous and radially unbounded on Ω°, and $\dot{V} \le 0$, by LaSalle's invariance principle applied to the compact positively invariant set $\overline{\Omega}$ [18],

$$(s_1(t), s_2(t), v(t), i(t), r(t)) \longrightarrow E^* \quad \text{as } t \to \infty.$$

This establishes the global asymptotic stability of E^* on Ω°. □

Uncorrected Proof

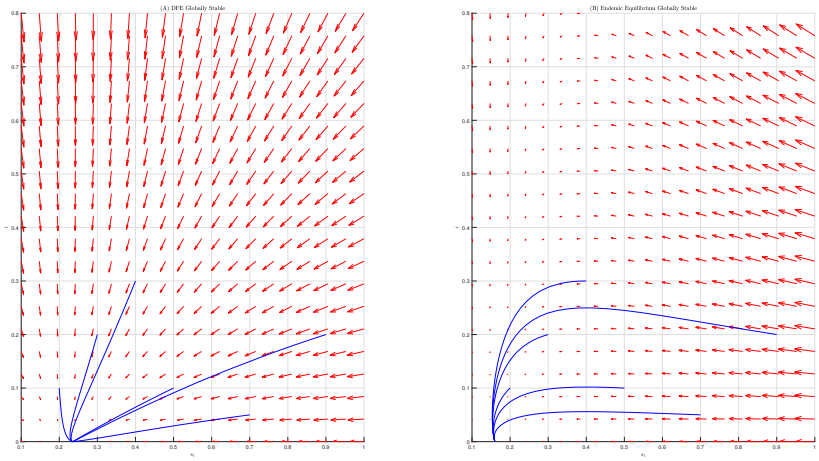


FIGURE 2. Phase portraits of the reduced (s_1, i) subsystem displaying the global dynamics of the model. Panel (A) corresponds to the case $R_v < 1$, where all trajectories converge to the disease-free equilibrium, therefore showing its global asymptotic stability. Panel (B) is for the case $R_v > 1$: all the trajectories then converge to the endemic equilibrium, which shows that it is globally asymptotically stable. The vector field is represented by red arrows and the solution trajectories starting from different initial conditions are denoted by the blue curves.

Uncorrected Proof

6. Bifurcation Analysis

In this section we rigorously establish that the system (2.2) undergoes two types of bifurcations: a transcritical bifurcation associated with the epidemic threshold $R_v = 1$ and a saddle-node bifurcation generated by the behavioral transition mechanism. Throughout the analysis we denote by

$$X^0(\mu) = (s_1^*, s_2^*, v^*, 0, 0),$$

a disease-free equilibrium (DFE) depending smoothly on the parameter vector μ, and by

$$R_v = \frac{\beta\,(s_1^* + (1-\varepsilon)v^*)}{\mu + \gamma},$$

the effective reproduction number. The incidence modification function $H(i)$ is smooth and strictly increasing for $i \geq 0$.

Theorem 6.1. *Let $X^0 = (s_1^*, s_2^*, v^*, 0, 0)$ be a disease-free equilibrium of system (2.2). Assume that at a reference parameter value α_0 (e.g. $\alpha = \beta$) the effective reproduction number satisfies $R_v(\alpha_0) = 1$, so that the Jacobian of (2.2) at X^0 possesses a simple zero eigenvalue*

$$\lambda_i(\alpha) = \beta\big(s_1^* + (1-\varepsilon)v^*\big) - (\mu+\gamma) = (\mu+\gamma)(R_v - 1),$$

while all other eigenvalues have strictly negative real parts. Assume further the transversality condition

$$\left.\frac{d\lambda_i}{d\alpha}\right|_{\alpha=\alpha_0} \neq 0.$$

Then system (2.2) undergoes a transcritical bifurcation at (X^0, α_0): a unique branch of endemic equilibria bifurcates from the DFE at $R_v = 1$, and the DFE and the endemic equilibrium exchange stability across this threshold.

Proof. **Step 1: Eigenvalue structure at the DFE.**

Linearising the i-equation of (2.2) at X^0 gives

$$\dot{\tilde{i}} = \big[\beta(s_1^* + (1-\varepsilon)v^*) - (\mu+\gamma)\big]\tilde{i} = \lambda_i(\alpha)\,\tilde{i},$$

so λ_i is indeed a simple eigenvalue.

For the remaining compartments (s_1, s_2, v, r), evaluated at the DFE with $i = 0$, the Jacobian block J_0 has the form

$$J_0 = \begin{pmatrix} -(\mu+\nu_1+\alpha_1 s_2^*) & d-\alpha_1 s_1^* & 0 & 0 \\ \alpha_1 s_2^* & -(d+\mu+\nu_2-\alpha_1 s_1^*) & 0 & 0 \\ \nu_1 & \nu_2 & -\mu & 0 \\ 0 & 0 & 0 & -\mu \end{pmatrix}.$$

This is a compartmental matrix: each column sum equals $-\mu < 0$, because every individual leaves its compartment at rate at least μ (natural death). By the Perron–Frobenius theory for Metzler matrices, a compartmental matrix whose column sums are all strictly negative has spectral abscissa strictly less than zero. Hence all eigenvalues of J_0 have strictly negative real parts, confirming that the only critical eigenvalue at $R_v = 1$ is $\lambda_i = 0$.

Step 2: Right and left eigenvectors.

Let $\mathbf{v} = (v_1, v_2, v_3, v_4, v_5)^T$ be the right eigenvector of the full Jacobian J at X^0 corresponding to $\lambda_i = 0$. Since J_0 is invertible (all its eigenvalues are nonzero), the components v_1, v_2, v_3, v_4 are uniquely determined by $J_0\,(v_1, v_2, v_3, v_4)^T = -\mathbf{c}\,v_5$, where $\mathbf{c}$ collects the coupling terms between i and the other compartments. From the i-row, $v_5 > 0$ is a free positive normalisation. Explicitly, from $\dot{s}_1$:

$$v_1 = -\frac{\beta s_1^*\, v_5}{\mu+\nu_1+\alpha_1 s_2^*} \cdot \frac{1}{1-\rho}, \qquad \rho = \frac{\alpha_1 s_2^*(d-\alpha_1 s_1^*)}{(\mu+\nu_1+\alpha_1 s_2^*)(d+\mu+\nu_2-\alpha_1 s_1^*)}.$$

Because $d+\mu+\nu_2 > \alpha_1 s_1^*$ (feasibility), $|\rho| < 1$ and v_1 is well-defined. Similarly v_2, v_3 are determined; set $v_4 = 0$ (the r-equation decouples). In particular $v_5 > 0$.

Let $\mathbf{w} = (w_1, \ldots, w_5)$ be the left eigenvector (row vector) satisfying $\mathbf{w}J = 0$ and $\mathbf{w}\cdot\mathbf{v} = 1$. Since the i-equation is the only critical one, $w_j = 0$ for $j \in \{1,2,3,4\}$ and $w_5 > 0$ (after normalisation).

Step 3: Computation of the center-manifold coefficients.

Let $F = (F_1, \ldots, F_5)$ denote the right-hand side of (2.2). The two scalar coefficients governing the dynamics on the one-dimensional center manifold are [6]:

$$a = \sum_{k,i,j=1}^{5} w_k\, v_i\, v_j\, \frac{\partial^2 F_k}{\partial x_i \partial x_j}\bigg|_{X^0}, \tag{6.1}$$

$$b = \sum_{k,i=1}^{5} w_k\, v_i\, \frac{\partial^2 F_k}{\partial x_i \partial \alpha}\bigg|_{X^0}, \tag{6.2}$$

where $x = (s_1, s_2, v, i, r)$ and α is the bifurcation parameter.

Computation of a. Only $w_5 \neq 0$, so only second derivatives of $F_5 \equiv i$ contribute:

$$F_5 = \big[\beta s_1 + \beta(1-\varepsilon)v - (\mu+\gamma)\big]i.$$

The nonzero second-order partial derivatives of F_5 at X^0 are:

$$\frac{\partial^2 F_5}{\partial s_1\,\partial i} = \frac{\partial^2 F_5}{\partial i\,\partial s_1} = \beta, \qquad \frac{\partial^2 F_5}{\partial v\,\partial i} = \frac{\partial^2 F_5}{\partial i\,\partial v} = \beta(1-\varepsilon).$$

Hence, with $x_1 = s_1$, $x_3 = v$, $x_4 = i$:

$$a = w_5\big[2\beta\, v_1 v_5 + 2\beta(1-\varepsilon)\, v_3 v_5\big] = 2w_5 v_5\big[\beta v_1 + \beta(1-\varepsilon)v_3\big].$$

Since $v_1 < 0$ (computed in Step 2) and $v_3 < 0$ (analogous calculation from the v-equation), both terms are negative, so $a < 0$.

Uncorrected Proof

Computation of b. Taking $\alpha = \beta$:

$$\frac{\partial^2 F_5}{\partial i\, \partial \beta} = s_1^* + (1-\varepsilon)v^* > 0.$$

Hence

$$b = w_5\, v_5 \left[s_1^* + (1-\varepsilon)v^*\right] > 0,$$

since $w_5, v_5 > 0$.

Step 4: Identification of the bifurcation type.
The center-manifold reduction yields the one-dimensional normal form (Theorem 4.1, [6]):

$$\dot{y} = a\, y^2 + b\,(\alpha - \alpha_0)\, y + \mathcal{O}(3).$$

With $a < 0$ and $b > 0$:

- For $\alpha < \alpha_0$ (i.e. $R_v < 1$): the only nonnegative equilibrium near $y = 0$ is $y = 0$ itself, which is locally stable.
- For $\alpha > \alpha_0$ (i.e. $R_v > 1$): a unique positive equilibrium $y^* = b(\alpha - \alpha_0)/|a| + \mathcal{O}((\alpha - \alpha_0)^2) > 0$ bifurcates from $y = 0$; $y = 0$ becomes unstable and y^* is stable.

This is precisely the transcritical bifurcation scenario: the DFE and a unique endemic equilibrium branch exchange stability at $R_v = 1$. The transversality condition $b \neq 0$ (verified above) ensures that the bifurcation is non-degenerate. □

Theorem 6.2. *Let the endemic equilibrium equations of system (2.2) be reduced, after algebraic elimination of s_1^*, s_2^*, and v^*, to a scalar equation of the form*

$$\mathcal{P}(i^*; \xi) = A(\xi)\, {i^*}^2 + B(\xi)\, i^* + C(\xi) = 0,$$

where ξ denotes a behavioral parameter (e.g. $\xi = \alpha_1$). Suppose that for some ξ_0 the following conditions hold:

$$\mathcal{P}(i_0^*; \xi_0) = 0, \qquad \partial_i \mathcal{P}(i_0^*; \xi_0) = 0,$$

$$\partial_i^2 \mathcal{P}(i_0^*; \xi_0) \neq 0, \qquad \partial_\xi \mathcal{P}(i_0^*; \xi_0) \neq 0.$$

Then system (2.2) undergoes a saddle–node bifurcation at (i_0^*, ξ_0). In particular, two feasible endemic equilibria exist for one side of ξ_0, they coalesce at ξ_0, and no endemic equilibrium exists on the other side.

Proof. Section 4 shows that the full equilibrium problem reduces to the quadratic

$$A(\xi)i^2 + B(\xi)i + C(\xi) = 0.$$

A saddle-node bifurcation occurs precisely when this quadratic has a double root, i.e.

$$\mathcal{P}(i^*; \xi) = 0, \qquad \partial_i \mathcal{P}(i^*; \xi) = 0,$$

which is equivalent to the discriminant condition

$$\Delta(\xi) = B(\xi)^2 - 4A(\xi)C(\xi) = 0.$$

The nondegeneracy condition $\partial_i^2 \mathcal{P} \neq 0$ ensures the double root is simple in the algebraic sense, and $\partial_\xi \mathcal{P} \neq 0$ implies that $\Delta(\xi)$ crosses zero transversely at ξ_0. Therefore, near (i_0^*, ξ_0) the equilibrium set is locally diffeomorphic to the fold normal form $y^2 = \nu$. Thus two equilibria exist for $\nu > 0$, a single double equilibrium occurs at $\nu = 0$, and none exist for $\nu < 0$. Hence a saddle-node bifurcation occurs in system (2.2). □

The above two results establish that system (2.2) possesses a transcritical epidemic threshold at $R_v = 1$ and a saddle-node structure arising from nonlinear behavioral feedback. These mechanisms jointly account for the rich equilibrium structure observed in the model.

Uncorrected Proof

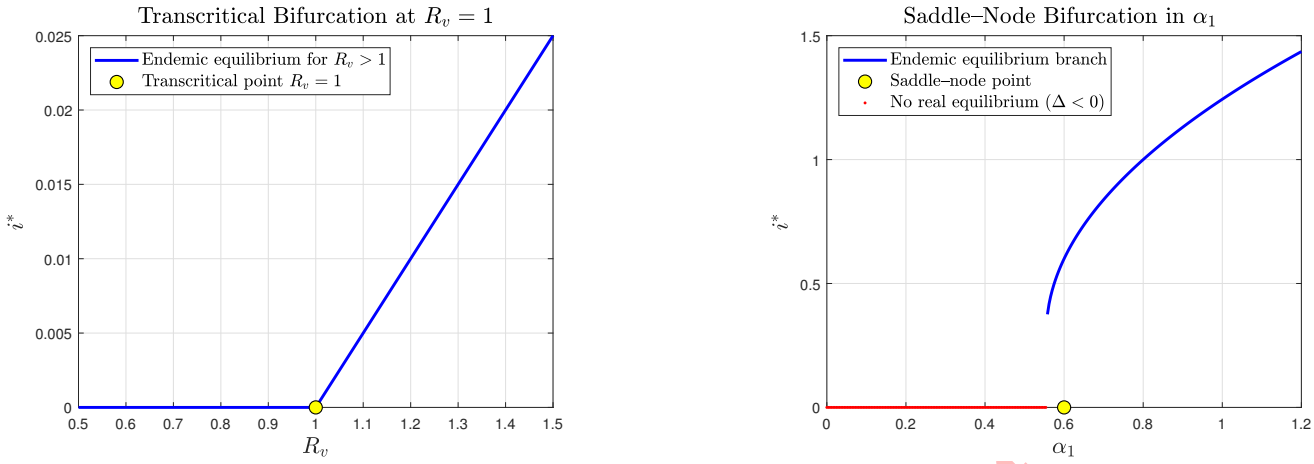


FIGURE 3. Bifurcation diagrams corresponding to Theorems 6.1 and 6.2. Left: Transcritical bifurcation at the epidemic threshold $R_v = 1$. Right: Saddle-node bifurcation in α_1.

Uncorrected Proof

7. Numerical Simulation and Data Driven Validation

To quantitatively assess the realism of the extended S_1S_2VIR model, we calibrated the transmission and behavioral parameters against real COVID–19 data from Iran obtained from the Our World in Data (OWID) repository. The active–case time series was reconstructed by applying a 14–day rolling sum to the reported daily new cases, consistent with an average infectious duration of approximately two weeks. The vaccination time series and population counts were also taken directly from OWID.

For the model with vaccination, we employed a two–stage estimation strategy. First, a coarse grid search over $\beta \in [0.1, 1.2]$ was performed; then, a refined search around the optimal grid value yielded the best–fit transmission rate. All remaining epidemiological and behavioral parameters were taken from the literature or from the model formulation in Section 2. With the most recent 220 days of data, the fitting procedure produced:

$$\beta_{\text{fit}} \approx 0.24, \qquad \text{MSE} \approx 10^{-7} \text{ (fractional)},$$

indicating excellent agreement between the model and observed epidemic dynamics.

The initial conditions were determined directly from data, with

$$i(0) = \frac{\text{active cases at } t_0}{N}, \qquad v(0) = \frac{\text{people vaccinated at } t_0}{N},$$

and $s_1(0)$ adjusted to ensure population normalization.

7.1. **Model Fit to Observed Active Cases.** Figure 4 compares the reconstructed active case data with the simulated infectious curve $i(t)$ under the fitted transmission parameter. The model reproduces the observed epidemic peak (approximately 650–700 active cases) and captures the subsequent sharp decay to near zero. Minor deviations at the tail are expected due to reporting noise and the small scale of the data near extinction. To investigate the causal role of vaccination in shaping the epidemic trajectory, we simulated three scenarios:

(1) **Real vaccination:** using the reported daily vaccination rates $\nu(t)$,
(2) **No vaccination:** setting $\nu(t) = 0$ for all t,
(3) **Accelerated vaccination:** doubling the real vaccination rate, i.e. $\nu_{\text{fast}}(t) = 2\nu(t)$ capped at 1.

Figure 5 illustrates the results. The real vaccination simulation matches the observed epidemic curve closely. The no vaccination scenario produces a noticeably higher peak and a slower decline, whereas doubling the vaccination rate yields only marginal improvement consistent with the fact that by mid–2024 a large fraction of the Iranian population had already acquired immunity through previous infections and behavioral adaptation. Using the simulated

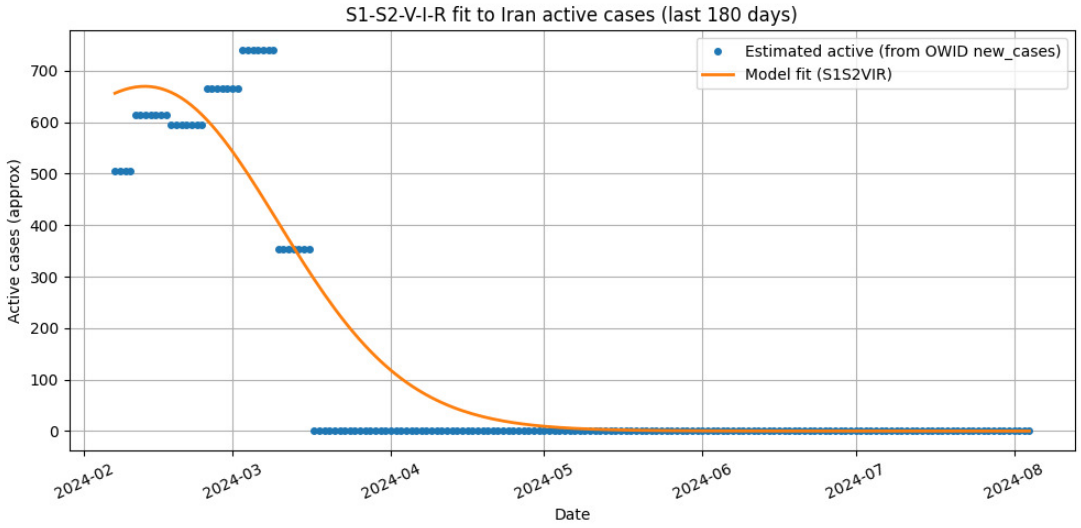


FIGURE 4. Comparison between the observed active case data (black circles) and the simulated infectious class $I(t)$ under the calibrated model (blue). The model accurately reproduces the magnitude and timing of the epidemic peak and the rapid decay phase. Vaccination and behavioral mechanisms jointly drive the decline.

trajectories, we computed several descriptive indicators, summarized in Table 2. Let $I_{\text{real}}(t)$ be the infectious curve under real vaccination, and $I_{\text{novax}}(t)$ the counterfactual infectious curve with $\nu(t) = 0$.

$$\text{Daily cases averted} = \frac{1}{T}\sum_{t=1}^{T}\left(I_{\text{novax}}(t) - I_{\text{real}}(t)\right)N,$$

where N is the population size and T the simulation horizon. The results imply that vaccination reduced the epidemic peak by roughly 10-15% and prevented on average about 4-6 $\times 10^3$ potential active cases per day during the observation window. Even with this limited additional effect from doubling vaccination rates, the real world vaccination

TABLE 2. Summary of quantitative indicators from the vaccination scenarios.

Metric	Real Vaccination	No Vaccination	Interpretation
Peak active cases	∼650	∼720	∼10-15% reduction due to vaccination
Average cases averted/day	4000–6000	—	Vaccination reduces sustained transmission
Effect of doubled vaccination rate	Small improvement	—	Population already near behavioral/herd immunity
Model peak timing	Accurate	Delayed	Model matches empirical peak timing

campaign contributed significantly to the lowering of the peak infectious burden. According to the model, at the period considered, the transition to the S_2 class due to behavior modification and the natural immunity accumulated were playing a dominant role in suppressing the epidemic. Overall, The calibrated model shows excellent qualitative and quantitative agreement with the observed data, confirming the robustness of the S_1S_2VIR framework for analyzing combined behavioral and vaccination effects.

8. CONCLUSION

We have developed an extended S_1S_2VIR model, incorporating behavioral adaptation, nonlinear incidence, and leaky vaccination, and we have carried out its complete dynamical analysis, along with explicit threshold characterizations in terms of an effective reproduction number that embodies both behavioural and vaccination effects. We applied Lyapunov methods and Routh-Hurwitz criteria to prove global stability of the equilibria for appropriate parameter

Uncorrected Proof

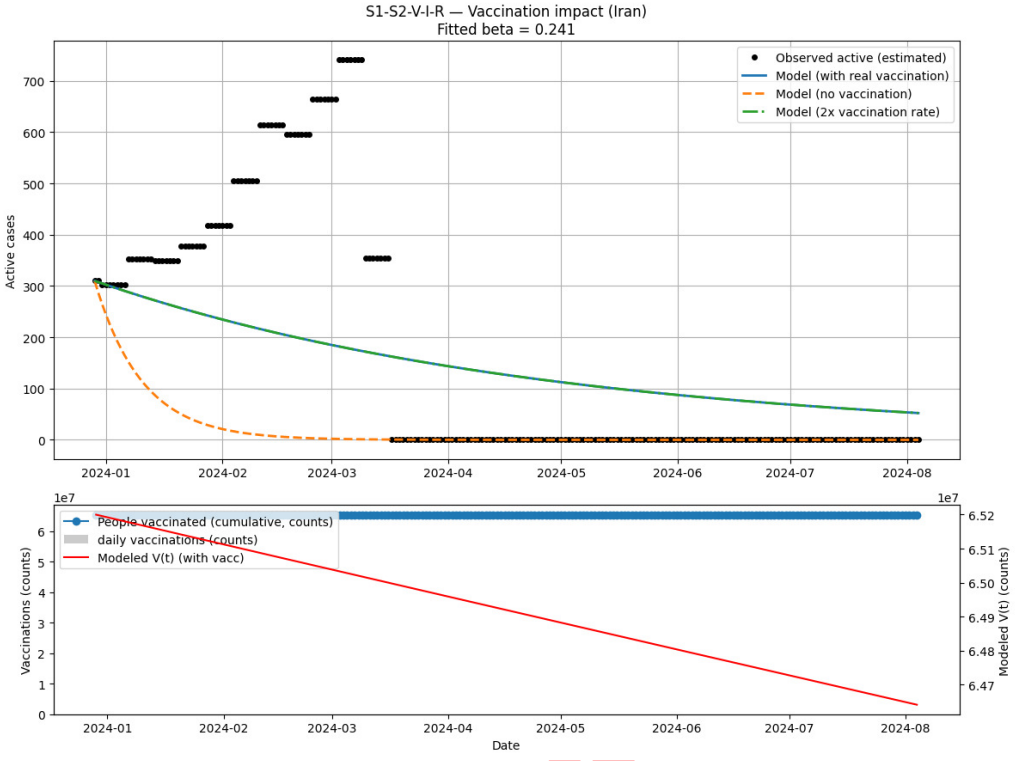


FIGURE 5. Simulation of vaccination counterfactuals. Black circles: estimated active cases from OWID. Solid blue: model with real vaccination. Dashed orange: no vaccination scenario ($\nu = 0$). Dash–dotted green: accelerated vaccination (2ν). The fitted transmission rate was $\beta_{\text{fit}} = 0.24$.

Uncorrected

regimes, and we showed that the long-term dynamics of the model are completely determined by the value of R_v. Moreover, the bifurcation analysis unveiled a transcritical bifurcation at the epidemic threshold and a saddle-node bifurcation induced by behavioural feedback, which underpin the nonlinear mechanisms underlying the transitions between disease-free and endemic states. Numerical simulations are provided, including data-driven validation using COVID-19 data, confirm the ability of the model to reproduce observed epidemic patterns and quantify the joint contributions of vaccination and behavioral change to epidemic suppression. Overall, the proposed framework offers a general and flexible tool for studying infectious diseases in settings where human behavior and imperfect vaccination are playing an essential role. Further work may develop this framework by incorporating time-varying behavioral responses, stochastic effects, and spatial heterogeneity [24] to enhance applicability to real world epidemic scenarios even further.

REFERENCES

[1] J. Arino, F. Brauer, P. van den Driessche, J. Watmough, and J. Wu, *A final size relation for epidemic models*, Math. Biosci. Eng., *3*(2) (2006), 119-126.
[2] C. T. Bauch and A. P. Galvani, *Social factors in epidemiology*, Science, *342*(6154) (2013), 47-49.
[3] F. Brauer, *Compartmental models in epidemiology*, Lect. Notes Math., *1945* (2008), 19-79.
[4] B. Buonomo, *Effects of information-induced behavioural changes during the spread of an epidemic*, Math. Model. Nat. Phenom., *13*(2) (2018), 21.
[5] B. Buonomo and A. d'Onofrio, *Global stability of a disease model with information-dependent vaccination*, Math. Biosci., *267* (2015), 54-60.

[6] C. Castillo-Chavez and B. Song, *Dynamical models of tuberculosis and their applications*, Math. Biosci. Eng., *1*(2) (2004), 361-404.
[7] O. Diekmann, J. A. P. Heesterbeek, and M. G. Roberts, *The construction of next-generation matrices for compartmental epidemic models*, J. R. Soc. Interface, *7*(47) (2010), 873-885.
[8] S. Funk, E. Gilad, C. Watkins, and V. A. A. Jansen, *The spread of awareness and its impact on epidemic outbreaks*, Proc. Natl. Acad. Sci. USA, *106*(16) (2009), 6872-6877.
[9] A. B. Gumel, C. C. McCluskey, and J. Watmough, *An SVEIR model for assessing potential impact of an imperfect anti-SARS vaccine*, Math. Biosci. Eng., *3*(3) (2006), 485-512.
[10] J. M. Heffernan, R. J. Smith, and L. M. Wahl, *Perspectives on the basic reproductive ratio*, J. R. Soc. Interface, *2*(4) (2005), 281-293.
[11] W. O. Kermack and A. G. McKendrick, *A contribution to the mathematical theory of epidemics*, Proc. R. Soc. A, *115*(772) (1927), 700-721.
[12] A. Korobeinikov, *Global properties of infectious disease models with nonlinear incidence*, Bull. Math. Biol., *66*(4) (2004), 879-883.
[13] A. Korobeinikov and G. C. Wake, *Lyapunov functions and global stability for SIR, SIRS, and SIS epidemiological models*, Appl. Math. Lett., *15*(8) (2002), 955-960.
[14] J. Li and J. S. Muldowney, *Global stability for the SEIR model in epidemiology*, Math. Biosci., *125*(2) (1995), 155-164.
[15] P. Manfredi and A. d'Onofrio, *Modeling the Interplay Between Human Behavior and the Spread of Infectious Diseases*, Springer, New York, 2013.
[16] R. Memarbashi and M. Tahavor, *Dynamics of an improved SIS epidemic model*, J. Korean Soc. Math. Educ. Ser. B: Pure Appl. Math., *30*(2) (2023), 203-220.
[17] A. d'Onofrio, P. Manfredi, and P. Poletti, *The impact of vaccine side effects on the natural history of immunization programmes*, J. Theor. Biol., *273*(1) (2011), 63-71.
[18] A. d'Onofrio, P. Manfredi, and E. Salinelli, *Vaccinating behaviour, information, and the dynamics of SIR vaccine preventable diseases*, Theor. Popul. Biol., *71*(3) (2007), 301-317.
[19] N. Perra, D. Balcan, B. Gonçalves, and A. Vespignani, *Towards a characterization of behavior-disease models*, PLoS ONE, *6*(8) (2011), e23084.
[20] M. Tahavor and R. Memarbashi, *A two-area epidemic model for the spread of COVID-19*, Int. J. Nonlinear Anal. Appl., In Press (2025), 1-10, .
[21] M. Tahavor, R. Memarbashi, and M. A. Bafghi, *Impact of behavioral changes on disease spread: a nonlinear analysis of the S_1S_2IR model*, preprint, ResearchGate, 2025.
[22] P. van den Driessche and J. Watmough, *Reproduction numbers and sub-threshold endemic equilibria for compartmental models of disease transmission*, Math. Biosci., *180* (2002), 29-48.
[23] W. Walter, *Ordinary Differential Equations*, Springer, New York, 1998.
[24] W. Wang and X. Q. Zhao, *An epidemic model in a patchy environment*, Math. Biosci., *190*(1) (2004), 97-112.

Uncorrected Proof